Influences of vegetation structure and elevation on CO_2 uptake in a mature jack pine forest in Saskatchewan, Canada

L. Chasmer, N. Kljun, A. Barr, A. Black, C. Hopkinson, H. McCaughey, and P. Treitz

Abstract: Carbon dioxide, water vapour, and energy fluxes vary spatially and temporally within forested environments. However, it is not clear to what extent they vary as a result of variability in the spatial distribution of biomass and elevation. The following study presents a new methodology for extracting changes in the structural characteristics of vegetation and elevation within footprint areas, for direct comparison with eddy covariance (EC) CO_2 flux concentrations. The purpose was to determine whether within-site canopy structure and local elevation influenced CO_2 fluxes in a mature jack pine (*Pinus banksiana* Lamb.) forest located in Saskatchewan, Canada. Airborne light detection and ranging (lidar) was used to extract tree height, canopy depth, foliage cover, and elevation within 30 min flux footprints. Within-footprint mean structural components and elevation were related to 30 min mean net ecosystem productivity (NEP) and gross ecosystem production (GEP). NEP and GEP were modeled using multiple regression, and when compared with measured fluxes, almost all periods showed improvements in the prediction of flux concentration when canopy structure and elevation were included. Increased biomass was related to increased NEP and GEP in June and August when the ecosystem was not limited by soil moisture. On a daily basis, fractional cover and elevation had varying but significant influences on CO_2 fluxes.

Résumé : French

[Traduit par la Rédaction]

Introduction

The eddy covariance (EC) method is commonly used to measure the direction and movement of energy and trace gas (e.g., water, CO_2) concentrations throughout ecosystems (Baldocchi 2008). Networks of EC systems have been set up at local, biome, continental, and global scales based loosely on the idea that individual nodes are representative of larger ecosystems. The data from these networks are then sometimes combined with remote sensing data and ecosystem models to determine spatial and temporal variability of CO_2 exchanges within areas that have undergone some prior disturbance (e.g., land management, extreme weather, insect infestation, fire, etc.), and within different stand ages, species types, and in areas of complex terrain (e.g., Heinsch et al. 2006).

Spatial heterogeneity in canopy structure and elevation may be an important consideration when measuring CO_2 and water fluxes, especially if wind directions do not vary. If the ecosystem is homogeneous, apart from other driving mechanisms, the location of the flux origin should not be important because it would not matter where the winds were originating from. There would be little variability in flux concentration because the characteristics of the ecosystem would be relatively similar in all directions. However, if the ecosystem is spatially variable, then flux concentrations may vary depending on spatial location and the dominant direction of the winds (Rahman et al. 2001;

Received 29 November 2007. Resubmitted 16 June 2008. Accepted 14 August 2008. Published on the NRC Research Press Web site at cjfr.nrc.ca on .

L. Chasmer,[1] H. McCaughey, and P. Treitz. Department of Geography, Queen's University, Kingston, ON K7L 3N6, Canada.
N. Kljun. Department of Geography, Swansea University, Swansea SA2 8PP, United Kingdom.
A. Barr. Climate Research Branch, Meteorological Service of Canada, Saskatoon, SK S7N 3H5, Canada.
A. Black. Faculty of Land and Food Systems, The University of British Columbia, Vancouver, BC V6T 1ZA, Canada.
C. Hopkinson. Applied Geomatics Research Group, Lawrencetown, NS BOS 1M0, Canada.

[1]Corresponding author (e-mail: lechasme@yahoo.ca).

doi:10.1139/X08-121

Fig. 1. (*a*) Lidar measured ground surface elevation within 750 m of the flux station with removal of understory and canopy vegetation. (*b*) Lidar measured canopy heights within 750 m of the flux station after removal of topographical influences. Blue circles represent the location of 11.3 m radius measurement plots, and the red circle represents the location of the eddy covariance flux tower (centre). Laser returns have been rasterized to produce a continuous surface digital elevation model (*a*) of the ground returns and a canopy height model of the maximum *z* returns (*b*).

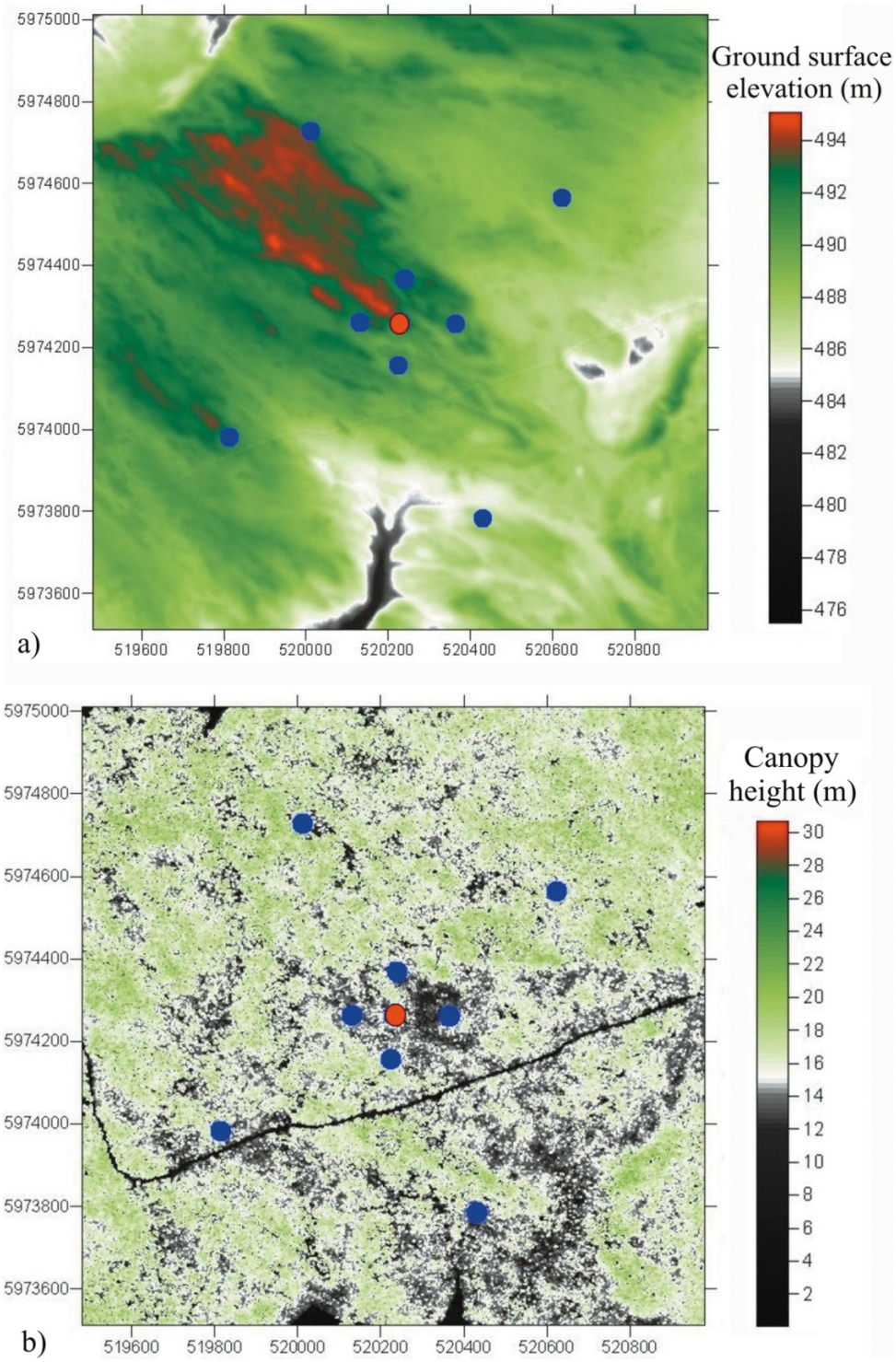

Chen et al. 2008). In many ecosystems, spatial variations in the availability of soil nutrients and moisture are manifested in the variability of aboveground biomass and exchanges measured by EC (Baldocchi and Meyers 1998; Griffis et al. 2003). If differences in the amount of CO_2 sequestration can be found among ecosystems, then is it true that variations in the amount of biomass may also affect CO_2 and water exchanges within a single ecosystem?

Table 1. Mean structural vegetation characteristics measured at eight plots surrounding the flux measurement station at the jack pine site.

Plot No.	UTM northing (zone 13) (m)	UTM easting (m)	Elevation (m)	DBH* (cm)	Tree height (m)	Canopy depth (m)†	LAIe‡ ($m^2 \cdot m^{-2}$)	Stem density (m^{-1})	Alder density (m^{-1})
1	520238.8	5974368.1	494.3	15.9	15.0	6.3	1.50	0.12	0.03
2	520224.5	5974155.5	495.1	14.6	13.6	6.1	1.45	0.08	0
3	520130.9	5974261.7	494.1	11.7	13.0	5.9	1.49	0.17	0
4	520365.4	5974259.0	492.5	12.9	13.3	5.2	1.55	0.15	0
5	520623.3	5974564.0	489.5	17.5	15.7	8.8	1.82	0.09	0.03
6	519813.4	5973981.9	491.9	16.1	14.9	8.1	1.52	0.10	0.02
7	520430.5	5973784.2	487.0	11.8	11.4	6.2	1.21	0.14	0
8	520012.7	5974728.1	492.4	23.6	16.4	11.2	1.49	0.04	0.47

*DBH, diameter at breast height.

†Canopy depth = canopy height – canopy base height.

‡LAIe, effective leaf area index.

Few studies have directly examined the influence of structural and elevation heterogeneity on fluxes within a single ecosystem (Kim et al. 2006; Chen et al. 2008). Until recently, measuring three-dimensional vegetation structure and ground surface elevation at high resolutions has been difficult. Airborne light detection and ranging (lidar) is an active remote sensing technology that is used to measure canopy structure and ground surface elevation at high resolution. A footprint model may then be used to discretize the variability in canopy structure and elevation at a particular place and time, which can then be correlated with trace gas exchanges measured by EC. The footprint model determines the probability that fluxes originated from a particular place within the ecosystem based on measured atmospheric turbulence (e.g., Foken and Leclerc 2004; Vesala et al. 2008). Each footprint therefore contains the extent in x and y coordinates of the source–sink area and a probability (probability density function (PDF)) that the CO_2 source–sink at x–y will be measured at the sensor.

In this study, vegetation structure and elevation were characterized using lidar within the contours of half-hourly flux footprint areas (approximately 80% of the probability of flux) from Kljun et al. (2004). The objective was to quantify the influences of vegetation structure and elevation on CO_2 concentrations measured by EC, specifically net ecosystem production (NEP) and gross ecosystem production (GEP). Three growing season periods were examined in 2002 at a mature jack pine (*Pinus banksiana* Lamb.) site in Saskatchewan, Canada.

Methods

Study area and site characteristics

The study area consists of a ≈90-year-old mature jack pine (OJP) forest (Baldocchi et al. 1997) located near the southern edge of the boreal forest (UTM coordinates: 520230 easting, 5974262 northing), Saskatchewan, Canada. The ground elevation varies between 482 and 494 m throughout the 1000 m radius surrounding the EC flux measurement tower, and tree heights vary by up to 6 m (Figs. 1*a* and *b*). The understory is composed of lichens (*Cladina* spp.), bearberry (*Arctostaphylos uva-ursi* L.), cranberry (*Vaccinium vitisideae* L.), and sparse groupings of alder (*Alnus crispa* Ait.). Soils within the site are coarse and well-drained sand with low nitrogen content (Baldocchi et al. 1997). Measurements of forest structure (e.g., canopy height) within eight geolocated forest mensuration plots were used to validate lidar canopy structural attributes within the ecosystem (Table 1).

Canopy structure measurements

Mensuration data (Table 1) were collected over two periods, 9 to 16 May and 25 July to 15 August 2005. Plot locations were selected for spatial representation according to compass cardinal directions at distances of 100 m (May field campaign) and 500 m (July–August field campaign) from the flux measurement station. Each plot has a radius of 11.3 m and follows Fluxnet-Canada protocols for measurements (Fluxnet-Canada 2003). Plot location, tree height, base of live crown height, diameter at breast height (DBH), gap fraction, and effective LAI (LAIe) were measured at each plot. Alder were also counted and measured for height and crown diameter in each cardinal direction. Plot centres were located using survey-grade, differentially corrected global positioning system (GPS) receivers (Leica SR530, Leica Geosystems Inc., Switzerland; Ashtec Locus, Ashtec Inc., Hicksville, New York) with the same base station coordinate as was used for the lidar survey. Geolocation accuracies varied from 1 cm to 1 m, depending on the density of the canopy cover at time of GPS data collection. Plots were geolocated so that lidar data could be directly compared with plot means and individual-tree measurements.

Canopy gap fraction was determined from digital hemispherical photography (DHP) at five locations within each plot (north, south, east, west, and centre), at distances of 11.3 m apart. All photographs were taken during diffuse daytime conditions, or 30 min before dawn or after dusk to reduce the influence of sun brightness and apparent leaf reduction within the photograph (Zhang et al. 2005). Photographs were exposed to two f-stops below automatic exposure (normally set between one and four exposure settings and with larger aperture) (Chen et al. 2006). Each individual photograph was processed following sky and vegetation thresholding methods of Leblanc et al. (2005) to obtain estimates of gap fraction and fractional cover (one-gap fraction). DHP version 1.6.1 software was used to process all photographs (S. Leblanc, Canada Centre for Remote Sensing provided to the Fluxnet-Canada Research Network).

LAIe estimates obtained with mean DHP measurements were 14% and 10% lower than estimates obtained by Chen

Fig. 2. Precipitation (millimetres) recorded at the mature jack pine study site during the 2002 growing season. Grey rectangles mark the duration of the three study periods. Total cumulative precipitation in 2002 is ~410 mm, which is the 30 year normal precipitation for this area, but 2002 was the second of two consecutive drought year in western Canada (Kljun et al. 2006).

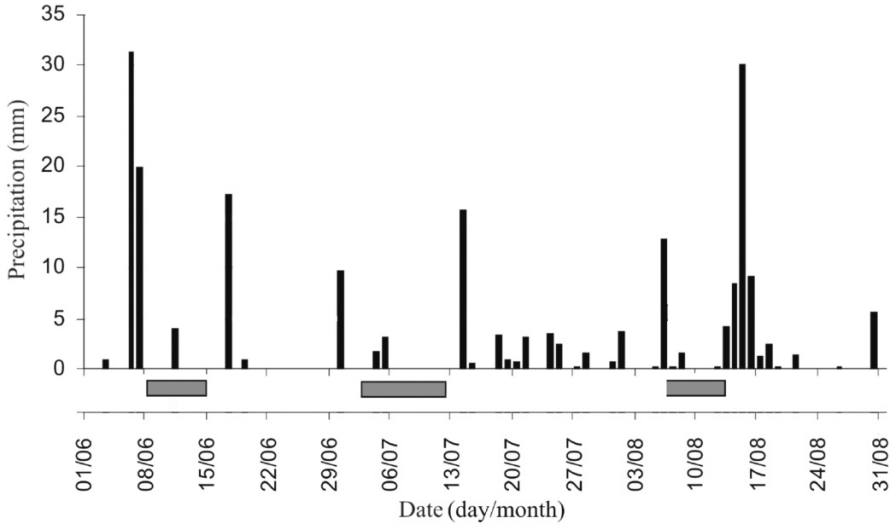

Fig. 3. A schematic diagram of the distribution of laser returns within a tree and the methods used to differentiate canopy height (90th percentile), canopy base height (8th percentile), canopy depth (canopy height – canopy base height), and f_{cover} within a 1 m × 1 m × z (height) column.

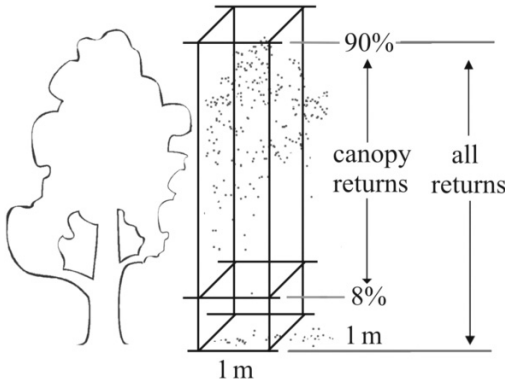

$$f_{cover} = \frac{\text{No. of returns between 90\% and 8\%}}{\text{No. of all returns}}$$

et al. (2006) at the same site with TRAC and LiCOR LAI-2000 transect methods, respectively. This variability in LAIe estimates was likely due to ecosystem heterogeneity within the study site and to technological differences between the optical methods of Chen et al. (2006) and the DHP method. Although our LAIe estimates differ from those of Chen et al. (2006), they provide reasonably close approximation of LAIe and, more importantly, are indicative of relative differences in canopy fractional cover using lidar.

Flux measurements

Meteorological, CO_2, and H_2O flux measurements at OJP have been collected for 30 min periods each day since 1999 (Griffis et al. 2003; Barr et al. 2006) and in 1994 during the Boreal Ecosystem–Atmosphere Study (BOREAS) (Middleton et al. 1997; Goetz et al. 1999). Three periods of five, nine, and seven days of flux and meteorological data were examined during the 2002 growing season when EC data were available. The selected periods occurred from 10 to 15 June (P1), 5 to 13 July (P2), and 7 to 13 August (P3) (see Fig. 2). These periods (and numbers of days) were chosen (1) to coincide with dry periods during which little to no rainfall occurred; and (2) so that the influence of three different soil moisture regimes could be examined. Mean tree height growth since BOREAS (1994 to 1996) measured in the field was approximately 1 m over an 11-year period (1994–2005) (Gower et al. 1997). Differences in canopy height between summer 2002 (flux measurements) and summer 2005 (field campaigns and lidar data collection) varied by less than 30 cm and were within the range of error of the lidar system.

Meteorological and flux measurements made at OJP are described in detail in Barr et al. (2006) and Kljun et al. (2006). Briefly, above-canopy CO_2 fluxes were measured approximately 28 m above the ground surface using the EC method at 20 Hz and aggregated over 30 min periods. A sonic anemometer (CSAT3, Campbell Scientific Inc., Edmonton, Alberta) and closed-path infrared gas analyzer (LI-6262, LI-COR Biosciences Inc., Lincoln, Nebraska) were used to measure friction velocity and atmospheric CO_2. Net ecosystem exchange (NEE) (micromoles per square metre per second) was measured by EC, where –NEE was equal to positive NEP (micromoles per square metre per second). A positive NEP indicates that greater amounts of CO_2 were used in photosynthesis than were released via ecosystem respiration (R_e). Daytime R_e (micromoles per square metre per second) was modeled from the relationship between nighttime R_e and soil temperature (Barr et al. 2006). GEP (micromoles per square metre per second), defined as the uptake of CO_2 by the ecosystem through photosynthesis, was estimated from measured NEP and modeled R_e, where GEP = NEP + R_e. A friction velocity threshold greater than 0.35 $m \cdot s^{-1}$ was used to filter out periods when wind speeds were too low for accurate estimates of flux concentration.

Uncertainties in measuring CO_2 fluxes occur because during calm and stable conditions the transfer of CO_2 by non-

Fig. 4. Daily 30 min footprint extent (80% contour lines) and wind direction for the three periods of study are overlaid onto the canopy height models for the mature jack pine study site (shown in Fig. 1*b*) to illustrate variability in canopy height and associated footprint locations for daytime periods (0900 to 1700 hours) (approximately 17 half-hourly periods or 8.5 h/day).

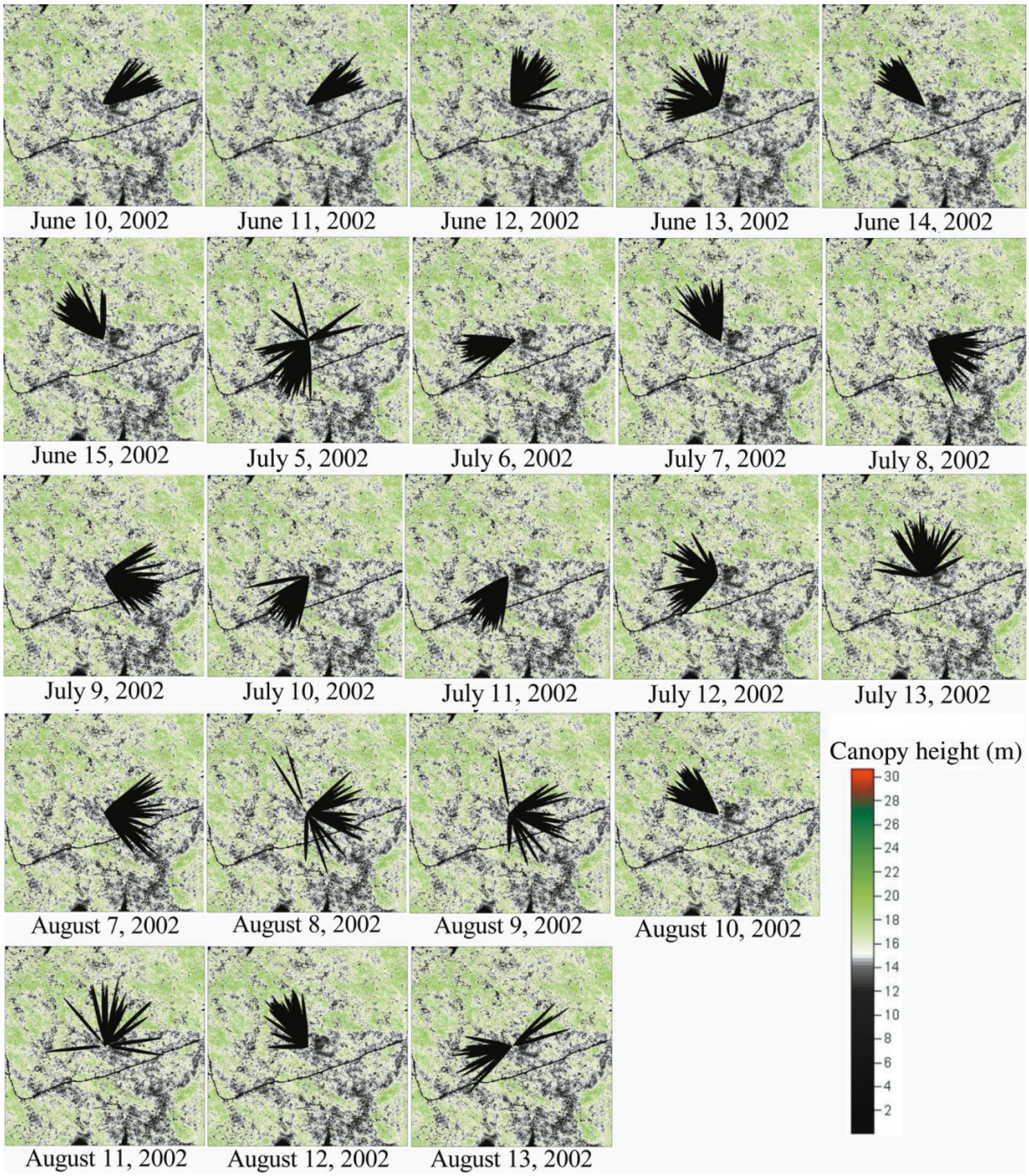

turbulent exchanges are not detected by the EC system (Massman and Lee 2002; Griffis et al. 2003). EC measurements obtained in early morning (before 0900 local sidereal time (LST)) and late afternoon (after 1700 LST) were not used to determined the relationship between CO_2 fluxes and canopy structure and site elevation because of the difficulty of measuring CO_2 storage in the air column below the EC sensors at those periods of the day (Yang et al. 1999). Nighttime fluxes were also excluded because during often stable nocturnal conditions the footprint source area sometimes extended beyond the lidar data set. Other issues associated with the accuracy of EC measurements include flux concentration loss due to (1) instrument setup limitations, (2) assumption of near-neutral atmospheric stability; (3) inability to consider the full complexity of EC equations; and (4) two-dimensional and thee-dimensional terrain influences (Massman and Lee 2002). The mean 24 h energy balance closure for each day and each period was determined using the energy balance ratio method (e.g., Wilson et al. 2002). Mean energy balance closure was ~88% for P1 (standard deviation (SD) = ~10%), ~83% for P2 (SD = ~8%), and ~85% for P3 (SD = ~14%), calculated from net radiation

Fig. 5. Wind roses of the percent frequency of wind directions at the mature jack pine study site during the year 2002 (*a*) and for the three periods studied (*b*).

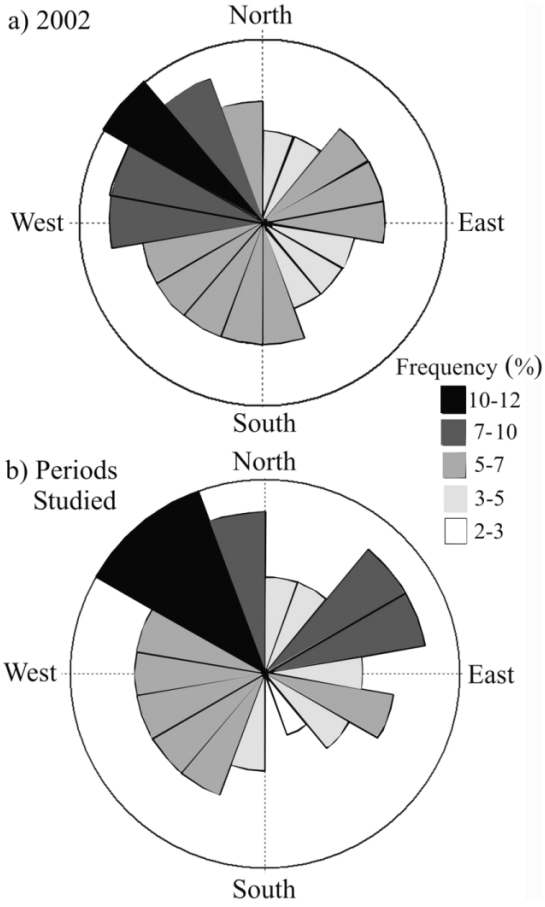

Table 2. Mean canopy structure characteristics and elevation surrounding the EC sensor for each wind-direction quadrants.

Wind-direction quadrants	Frequency of wind origin (%)*	Mean tree height (m)	Mean f_{cover}	Mean elevation (m)
Northwest	45	16.4	0.74	495
Southwest	20	14.9	0.55	491
Northeast	18	15.2	0.67	490
Southeast	17	11.6	0.43	487
Site mean	—	14.8	0.63	491

Note: Source of flux areas may be influenced differently depending on wind direction, canopy structure, and elevation.

*Mean values for the three periods studied.

(R_n), latent heat flux (Le), sensible heat flux (H), and soil heat flux (G). Barr et al. (2006) suggest that an energy balance correction may be applied to CO_2 fluxes so that they are increased relative to the percentage that is underestimated when unable to close the energy balance. This assumes that underestimated energy fluxes are representative of underestimated CO_2 fluxes. Based on this assumption, CO_2 fluxes have been corrected for underestimated energy fluxes and an inability to close the energy balance at OJP and other mature forest sites operated by Fluxnet-Canada (Canadian Carbon Program) at the Boreal Ecosystem Research and Monitoring Sites (BERMS).

Meteorological variables were also examined to determine the influence of meteorology on flux exchanges prior to examining canopy structure and elevation effects. Measurements included above canopy incoming photosynthetically active radiation (PAR, micromoles per square metre per second), relative humidity (RH, percentage), and air temperature (T_{air}, degrees Celsius) (model HMP45C, Vaisala by Campbell Scientific Inc., Edmonton Alberta); soil temperature (T_{soil}, degrees Celsius) (CS107b, Campbell Scientific Inc., Edmonton, Alberta); and volumetric soil moisture (θ, cubic metres per cubic metre) (CS615, Campbell Scientific Inc., Edmonton, Alberta). Above-canopy incoming and reflected PAR and below-canopy incoming PAR were measured using LI-COR model LI190 (LI-COR Biosciences, Nebraska). θ was measured at depths of 30 to 60 cm, and T_{soil} was measured at depths of 10 cm. RH and T_{air} were measured above the canopy at a height of 16 m.

Lidar data collection and processing

Lidar data were obtained at OJP on 12 August 2005 (Fig. 1) using a scanning discrete pulse return system (ALTM3100, Optech Inc., North York, Ontario). The ALTM3100 is owned and operated by the Applied Geomatics Research Group, Nova Scotia. Up to four laser pulse reflections or "returns" were obtained per laser pulse emitted, at a rate of 71 kHz and at a flying height of 950 m above ground level (a.g.l.). The scan angle was set at ±19° with 50% overlap of adjacent flight lines. This enabled penetration of laser pulses through to the base of the canopy, while also obtaining returns on all sides of individual trees (Chasmer et al. 2006). Cross-track and down-track resolutions, with 50% overlap of scans, were 35 cm ("post spacing", the distance between returns).

Percentile distributions were used to approximate mean tree heights, base of live crown height, and canopy depth (e.g., Lim and Treitz 2004; Chasmer et al. 2006) within footprint PDF contour lines. Height and live canopy base height percentile distributions were calculated on individual returns greater than or equal to 1.3 m above the ground surface so that returns from the ground surface would not influence and shift the percentiles downwards. Percentile distributions were also compared with plots measurements to determine the most accurate and descriptive percentiles to adopt. The 90th and 8th percentiles were most appropriate for determining mean tree height and base of live crown height at the plot level. The resulting values underestimated canopy heights by up to 0.94 m and overestimated the base of the live crown heights by up to 0.77 m when compared with plot-level means. Canopy fractional cover (f_{cover}) (where 1 = full canopy cover and 0 = no canopy cover) was determined from laser returns based on the ratio of the number of canopy returns to the number of canopy and ground returns:

$$[1] \qquad f_{cover} = \frac{\sum P_{canopy}}{\sum P_{all}}$$

where P_{canopy} is the total frequency of laser pulse returns within the canopy (≥1.3 m a.g.l.), and P_{all} is the total fre-

Fig. 6. Relationships between net ecosystem productivity (NEP) (*a*, *b*, and *c*) and gross ecosystem productivity (GEP) (*d*, *e*, and *f*), and photosynthetically active radiation (PAR) represented by Landsberg light response curves at the mature jack pine study site during the three periods of study: 10–15 June 2002 (*a* and *d*), 5–13 July 2002 (*b* and *e*), and 7–13 August 2002 (*c* and *f*). Relationships are shown for entire days when incoming PAR exceeded 0.1 μmol·m^{-2}·s^{-1}.

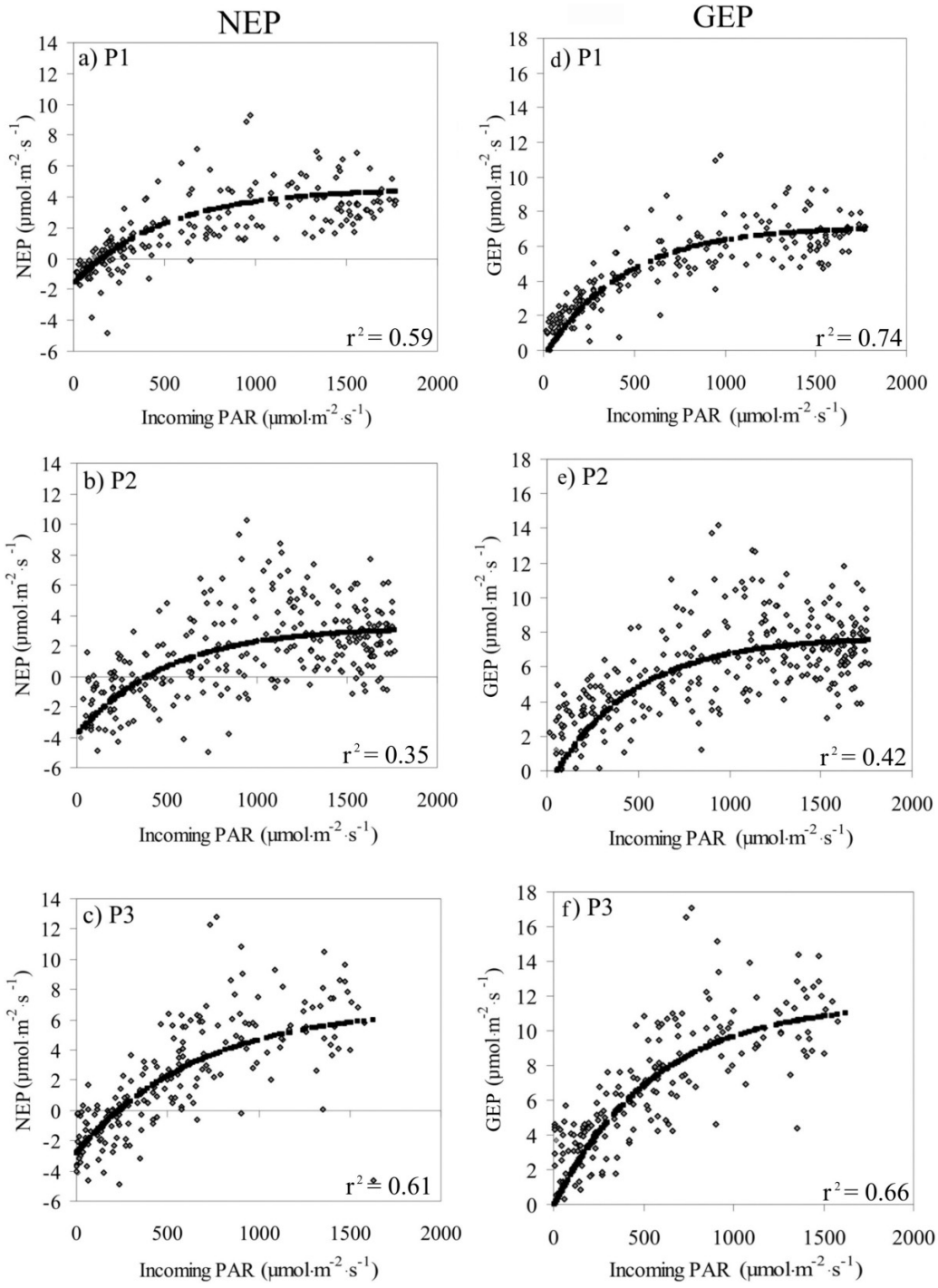

quency of all laser pulse returns from the canopy and ground surface within each 1 m × 1 m × 30 m column. A height of 1.3 m was chosen to capture the base of the canopy without including the understory, and also because the lidar is unable to record multiple returns at heights within approximately 1.3 m of the ground. Morsdorf et al. (2006) indicate that f_{cover} is an effective proxy indicator of variations in foliage density. A schematic diagram of the lidar structure classification is provided in Fig. 3.

Footprint data analysis

The footprint parameterization used in this study follows that of Kljun et al. (2004). This parameterization was chosen because (1) it is based on variables that are easy to derive from measurements obtained from EC; (2) it is neither

Table 3. Mean meteorological conditions and maximum net ecosystem productivity (NEP) and gross ecosystem productivity (GEP) at saturation (P_{max}) during three periods studied.

Periods	NEP P_{max} ($\mu mol \cdot m^{-2} \cdot s^{-1}$)	GEP P_{max} ($\mu mol \cdot m^{-2} \cdot s^{-1}$)	Mean θ ($m^3 \cdot m^{-3}$)	Mean T_{air} (°C)	Mean T_{soil} (°C)	Mean VPD (Pa)	Mean incoming PAR ($\mu mol \cdot m^{-2} \cdot s^{-1}$)
P1	4.5	7.1	0.82	16.8	9.2	132	767
P2	3.2	7.7	0.54	23.7	14.4	299	955
P3	6.8	11.6	0.068	19.0	14.3	154	523

Note: θ, volumetric soil moisture; T_{air}, air temperature; T_{soil}, soil temperature; VPD, vapor pressure deficit; PAR, photosynthetically active radiation.

computationally difficult nor time intensive; and (3) it has been thoroughly applied and tested using a variety of meteorological (e.g., varying stability, roughness length, etc.) and technological (instrument measurement height) applications (Kljun et al. 2004).

The footprint parameterization allows for the derivation of the crosswind-integrated footprint ($\bar{f}^y$) based on the along-wind distance from the EC (x), the EC height (z_m), roughness length (z_0), and the height of the planetary boundary layer (H). Directionality and origin of the flux were determined from wind direction. Trace gas advection and diffusion was accounted for in the surface friction velocity (u_*), whereas buoyancy and the formation and size of eddies within the planetary boundary layer were determined using the standard deviation of the vertical velocity (σ_w). Dispersion in the y direction (the crosswind distance from the centre line) was calculated using a Gaussian function (Amiro 1998). Roughness length (z_0) at OJP was estimated from Choudhury and Monteith (1988) as:

$$[2] \qquad z_0 = \begin{cases} z_{0s} + 0.28hX^{1/2} & \text{for } 0 \le X \le 0.2 \\ 0.3h\left(\dfrac{1-d}{h}\right) & \text{for } 0.2 \le X \le 2 \end{cases}$$

and

$$[3] \qquad d = h[\ln(1 + X^{1/6}) + 0.031 \ \ln(1 + X^6)]$$

where X = 0.2LAI (1.5 $m^2 \cdot m^{-2}$ on average at OJP), h is the mean height of the canopy, and z_{0s} is the soil surface roughness (= $0.10h_s$, where h_s is the height of the understory (Shuttleworth and Wallace 1985; Monteith and Unsworth 1990). The understory consisted mainly of sporadic and infrequently occurring alder, and in many cases footprints contained little to no understory, and therefore, h_s was assigned a value of zero. Finally, d is zero plane displacement. Therefore, at OJP z_0 was 1.9 m using the mean measured tree height of 14.2 m and varied between 1.6 m (for the shortest tree, 11.4 m) and 2.2 m (for the tallest tree, 16.4 m). The location of maximum daytime flux varied between 176 and 200 m from the flux tower for areas of smaller z_0 versus areas of higher z_0, respectively, whereas the along wind distance could vary by as much as 50 m. Because of these slight variations in roughness length and minimal impact on footprint size, mean z_0 for the entire site was based on mean tree height.

Variable wind speed and boundary layer height also affect the length of the footprint (not shown), where increased u_* and decreased H result in footprints located nearer to the EC. Richardson number (Ri) was used to determine approximate stability of the atmosphere (Monteith and Unsworth 1990) based on air temperature and wind speed at 30 min periods during relatively unstable conditions when u_* was >0.35 $m \cdot s^{-1}$:

$$[4] \qquad \mathrm{Ri} = \frac{(gT^{-1}\partial T_{air})/\partial z}{(\partial u/\partial z)^2}$$

where T is absolute temperature (degrees Kelvin), g is gravitational acceleration (9.8 $m \cdot s^{-1}$), u is wind speed, and z is height. The generalized stability factor is calculated as

$$[5] \qquad F = (1 - 5\mathrm{Ri})^2 \quad 0.1 \le \mathrm{Ri} \le 1$$

and

$$[6] \qquad F = (1 - 16\mathrm{Ri})^{0.75} \quad \mathrm{Ri} < -0.1.$$

F was used to approximate H following tables in Gryning et al. (1987). The maximum along-wind and crosswind distances were used to estimate the area of the footprint and within-footprint mean canopy structure and elevation characteristics. Canopy structure and elevation were then correlated with 30 min mean CO_2 flux concentrations measured by EC.

Statistical analysis

To determine whether vegetation structure and elevation affect NEP and GEP, the combined influences of meteorological variables were first examined. Meteorological variables included incoming PAR, RH, T_{air}, T_{soil}, and θ. A Landsberg light response curve (Landsberg and Waring 1997; Chen et al. 2002) was used to examine the relationship between incoming PAR and NEP (GEP) during individual periods:

$$[7] \qquad \mathrm{NEP} = P_{max}\ (1 - e^{-a(\mathrm{PAR} - I_{comp})})$$

where P_{max} is the maximum mean NEP (or GEP) at saturation, α is the slope of NEP (GEP) as it increases with incoming PAR, and I_{comp} is the light compensation point. The residuals of the measured versus modeled flux ($NEP_{measured} - NEP_{modelled}$) were then examined to determine the remaining contribution of the most important meteorological variables (RH, T_{soil}, and θ) to the variability in the flux. This was done using a multiple linear regression (Chen et al. 2002). A linear regression was chosen because it was best able to describe the variability in the residuals. A second multiple linear regression was also performed to examine the combined influences of meteorological variables and the most important canopy structure (f_{cover}) and elevation influences on the flux. Both multiple regression analyses were added (separately) to the $NEP_{modelled}$ and $GEP_{modelled}$ and compared

Table 4. Pearson's correlation coefficients for the relationships between net ecosystem productivity (NEP) and gross ecosystem productivity (GEP), and photosynthetically active radiation (PAR) using the Landsberg light response curve.

	Period	Incoming PAR	T_{air}	RH	T_{soil}	θ
NEP	P1	0.77 (0.000)	–0.59 (0.000)	0.54 (0.000)	–0.63 (0.000)	0.22 (0.02)
	P2	0.59 (0.000)	–0.66 (0.000)	0.57 (0.000)	–0.49 (0.000)	0.30 (0.000)
	P3	0.78 (0.000)	–0.25 (0.004)	–0.072 (0.41)	–0.20 (0.03)	0.02 (0.79)
GEP	P1	0.86 (0.000)	–0.45 (0.000)	0.46 (0.000)	–0.38 (0.000)	0.007 (0.94)
	P2	0.65 (0.000)	–0.63 (0.000)	0.58 (0.000)	–0.42 (0.000)	0.30 (0.000)
	P3	0.81 (0.000)	–0.25 (0.004)	0.03 (0.74)	–0.12 (0.19)	–0.02 (0.86)

Note: Dominant meteorological variables affecting the residuals of NEP and GEP after accounting for PAR are also included: T_{air}, air temperature; RH, relative humidity; T_{soil}, soil temperature; θ, volumetric soil moisture. The p values for the correlations between NEP and GEP, and the driving variables are given in brackets. Number of observations = 192 (P1), 288 (P2), and 224 (P3).

with the measured NEP and GEP for each time period. Pearson's r correlation was used to determine the relative correspondence between flux concentration and meteorological driving variables, canopy structure, and elevation as a correlation matrix.

The influence of local meteorology was also assessed by relating wind direction to meteorological driving variables during the periods of study. It could be argued that winds originating from particular directions may bring specific conditions (e.g., a wind originating from the north bringing cold air, a wind originating from the south bringing warm air, changes in humidity from nearby lakes, etc.). that could affect the local meteorological driving variables and photosynthesis. During the periods of study, wind direction had no influence on local meteorology. T_{air} ranged from $\sim$5 to 30 °C, and a two-sample t test confirms that T_{air} was unrelated to the origin of wind (r^2 = 0.04, p = 0.8). Similarly, RH also had no relationship to wind direction (based on a two-sample t test), and varied between $\sim$20% and 100%, regardless of wind origin (r^2 = 0.05, p = 0.72). Therefore, local weather conditions were not dependent on wind direction during the periods studied.

Results

Footprint climatologies

Half-hourly filled footprint contour lines during three periods of study were "overlaid" onto the canopy height models derived from lidar (Fig. 4) to illustrate footprint directionality and location within the ecosystem. The main part of the footprint (containing 80% probability of flux) occurred within 500 m of the EC system, whereas footprint areas often extended to 1 km and beyond during stable conditions. Figure 5 illustrates the frequency of wind directions and flux origins throughout 2002 and during three periods of study. During 2002, approximately 45% of fluxes originated from areas northwest of the EC system. Within these areas elevation, tree height, and leaf area were above the mean values for the site (Table 2). Fluxes from the southwest (20%) and the northeast (18%) originated from areas where vegetation structure characteristics and elevation were average. Seventeen percent of winds originated from southeast quadrants, which typically had lower elevations, shorter trees, and lower leaf area. If winds originated from some directions more than others, the EC system may not have adequately sampled all of the within-site heterogeneity in fluxes. By comparison, during the three periods studied (Fig. 5*b*), fluxes tended to come from wind directions that were fairly representative of the dominant directions for 2002. Sampling from most directions allowed for comparisons to be made among most parts of the ecosystem, bearing in mind that fluxes throughout the year most frequently originated from the northwest.

Dominant meteorological driving variables

To determine the relationship between fluxes and spatial variability in biomass and elevation, the influence of meteorological variables on CO_2 uptake needs to first be determined so that structural and spatial influences can be separated from those attributable to changing meteorological conditions. During all three periods, meteorological variables had varying influences on CO_2 fluxes. Landsberg light response curves indicate that NEP and GEP saturated at different levels of PAR depending on the time period within the growing season and available θ (Fig. 6). The amount of precipitation received before the periods studied was higher for P1 and P3 than for P2, and P2 had higher T_{air} than the other two periods. Saturation of NEP and GEP was more pronounced during P1 and P2 and was increasingly linear during P3. Table 3 provides information on mean meteorological conditions per period, incoming PAR, θ, T_{air}, and the vapor pressure deficit, all of which likely affected NEP and GEP light response curves during the three periods of study.

Saturation of photosynthesis at OJP was consistent with the results of Turner et al. (2003). These authors found that two forests (one conifer and one deciduous) tended to saturate at high levels of absorbed PAR because of the low photosynthetic capacity of shade leaves and possible inhibition of photosynthesis of sunlit leaves during the afternoon. Within-season influences of incoming PAR on CO_2 uptake and lower rates of saturation during P3 (as opposed to P1 and P2) were also found in Hollinger et al. (1999) in a mixed forest. Middleton et al. (1997) found that lower water use efficiency, reduced evapotranspiration, and reduced CO_2 uptake at OJP in June and July 1994 were caused by low soil moisture and stomatal limitations to photosynthesis. They also observed a late summer – early autumn peak in photosynthesis at OJP and attributed this to the maturing of new needles. New needles commence growth in June and

Table 5. Pearson's r correlation matrix of interacting meteorological driving variables and p values (in parentheses).

Period		Incoming PAR	T_{air}	RH	T_{soil}	θ
P1	Incoming PAR	—	0.59 (0.000)	–0.60 (0.000)	0.09 (0.19)	–0.23 (0.002)
	T_{air}	0.59 (0.000)	—	–0.94 (0.000)	0.65 (0.000)	–0.42 (0.000)
	RH	–0.60 (0.000)	–0.94 (0.000)	—	–0.62 (0.000)	0.34 (0.000)
	T_{soil}	0.09 (0.19)	0.65 (0.000)	–0.62 (0.000)	—	–0.67 (0.000)
	θ	–0.23 (0.002)	–0.42 (0.000)	0.34 (0.000)	–0.67 (0.000)	—
P2	Incoming PAR	—	0.42 (0.000)	–0.51 (0.000)	–0.13 (0.03)	0.09 (0.1)
	T_{air}	0.42 (0.000)	—	–0.69 (0.000)	0.68 (0.000)	–0.46 (0.000)
	RH	–0.51 (0.000)	–0.69 (0.000)	—	–0.15 (0.01)	–0.08 (0.18)
	T_{soil}	–0.13 (0.03)	0.68 (0.000)	–0.15 (0.01)	—	–0.80 (0.000)
	θ	0.09 (0.1)	–0.46 (0.000)	–0.08 (0.18)	–0.80 (0.000)	—
P3	Incoming PAR	—	0.50 (0.000)	–0.59 (0.000)	–0.10 (0.16)	0.33 (0.000)
	T_{air}	0.50 (0.000)	—	–0.56 (0.000)	0.45 (0.000)	0.22 (0.001)
	RH	–0.59 (0.000)	–0.56 (0.000)	—	–0.50 (0.000)	–0.61 (0.000)
	T_{soil}	–0.10 (0.16)	0.45 (0.000)	–0.50 (0.000)	—	0.18 (0.007)
	θ	0.33 (0.000)	0.22 (0.001)	–0.61 (0.000)	0.18 (0.007)	—

Note: PAR, photosynthetically active radiation; T_{air}, air temperature; RH, relative humidity; T_{soil}, soil temperature; θ, volumetric soil moisture.

Table 6. Landsberg and multiple regression equations used to predict net ecosystem productivity (NEP) and gross ecosystem productivity (GEP) using meteorological variables.

				p value of contribution		
	Period	Landsberg equation	Multiple regression equation	RH	T_{soil}	θ
NEP	P1	$y = 4.5(1 - e^{-0.002(PAR-160)})$	$NEP_r = 23.9 + 0.016RH - 1.55\ T_{soil} - 129\theta$	0.001	0.000	0.000
	P2	$y = 3.2(1 - e^{-0.002(PAR-400)})$	$NEP_r = -14.8 - 0.04RH + 0.92T_{soil} + 58.9\theta$	0.000	0.000	0.390
	P3	$y = 6.8(1 - e^{-0.0015(PAR-235)})$	$NEP_r = -22.8 + 0.02RH - 1.06T_{soil} - 85\theta$	0.039	0.005	0.816
GEP	P1	$y = 7.1(1 - e^{-0.0023(PAR-32)})$	$GEP_r = 3.10 + 0.01RH - 0.23T_{soil} - 17.7\theta$	0.006	0.439	0.202
	P2	$y = 7.7(1 - e^{-0.0022(PAR-60)})$	$GEP_r = -8.4 + 0.05RH - 0.06T_{soil} + 139\theta$	0.000	0.769	0.051
	P3	$y = 11.6(1 - e^{-0.0018(PAR-10)})$	$GEP_r = 16.7 + 0.005RH - 0.49T_{soil} - 140\theta$	0.687	0.183	0.656

Note: PAR, photosynthetically active radiation; RH, relative humidity; T_{soil}, soil temperature; θ, volumetric soil moisture. The relative importance of each contribution is indicated by the p value. Number of observations = 111 (P1), 166 (P2), and 126 (P3).

are fully developed by mid-July, enabling increased photosynthesis in August (Middleton et al. 1997).

Incoming PAR accounted for the greatest variability in NEP and GEP during the three periods studied (Table 4) but had the least influence during P2 when NEP and GEP were highly variable. After removing the influence of PAR on NEP and GEP using the Landsberg equation, the residuals of the variance of NEP and GEP were affected by T_{air}, RH, θ, and T_{soil} to varying degrees. Table 4 summarizes the relationships and significance between the driving variables and NEP and GEP, respectively, during the three periods studied.

Interacting influences between meteorological variables and CO_2 fluxes cannot be ignored (Chen et al. 2002). Incoming PAR, T_{air}, RH, T_{soil}, and θ all covaried with each other to some degree, resulting in similar combined influences on NEP and GEP, as described in a correlation matrix during the three periods in Table 5. Incoming PAR correlated strongly with RH, to a lesser extent with T_{air}, and very little with T_{soil} and θ. T_{air} also correlated strongly with RH and T_{soil}, whereas RH correlated less strongly with T_{soil}. If each variable is assessed individually with the residuals of NEP and GEP, after removing the influence of incoming PAR, T_{air} and RH typically have similar but opposite influences on the residuals (Table 4). This result suggests that T_{air} was typically low and RH was high when NEP and GEP residuals were positive (i.e., when the Landsberg equation underestimated NEP and GEP). T_{soil} and θ also had similar relationships with NEP and GEP residuals, but they were not as pronounced as those of T_{air} and RH (Table 4). The influence of T_{soil} was similar to that of T_{air}, and T_{soil} was negatively related to increases in NEP and GEP residuals during all periods, whereas θ had the opposite relationship with the residuals (i.e, T_{soil} was low, and θ had greater water content during periods of increased CO_2 uptake). Similar results were also found at three Douglas-fir (*Pseudotsuga menziesii* (Mirb.) Franco) sites of varying ages in Chen et al. (2002), where T_{soil} and T_{air} were also negatively related to increases in the residuals of NEP (increased temperature equals decreased NEP).

Meteorological variables RH, T_{soil}, and θ were combined using a multiple linear regression with the residuals of incoming PAR from the Landsberg approach (Table 6). These variables were used because there was the least interaction between them and they described the greatest combined variability in CO_2 flux. RH was able to describe much of the variability in T_{air}, resulting in the exclusion of T_{air} from the analysis. T_{soil} was included, and even though it was used to derive GEP, it did not greatly covary with GEP during the periods examined (r = –0.02 for P1; –0.36 for P2; –0.18

Fig. 7. Relationships (adjusted r^2) between net ecosystem productivity (NEP) (*a*, *b*, and *c*), gross ecosystem productivity (GEP) (*d*, *e*, and *f*), and modeled estimates obtained using the Landsberg equation and multiple regression of the residuals presented in Table 6 during the three periods of study: 10–15 June 2002 (*a* and *d*), 5–13 July 2002 (*b* and *e*), and 7–13 August 2002 (*c* and *f*). Relationships are shown for entire days when incoming photosynthetically active radiation (PAR) exceeded 0.1 μmol·m^{-2}·s^{-1}.

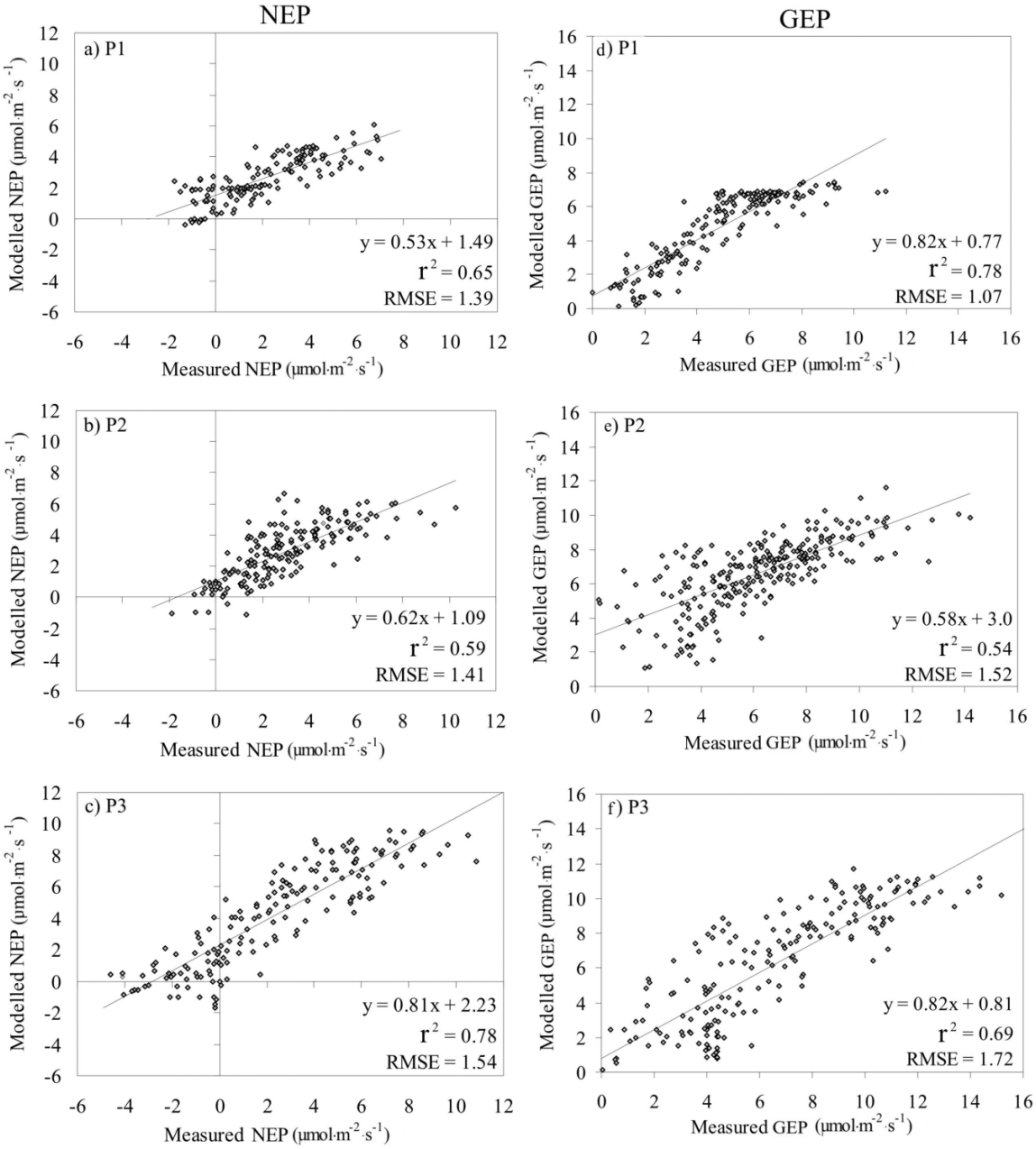

for P3). The multiple regressions were performed on the residuals of PAR versus NEP and GEP for each study period because the Landsberg curve provided the best description of the relationship (Table 6). Regression equations were then added to the Landsberg equation for each study period and were plotted against measured NEP and GEP in Fig. 7. In all cases, inclusion of meteorological driving variables (apart from incoming PAR) improved the prediction of NEP and GEP.

Within-footprint vegetation structural and elevation influences on CO_2 Fluxes

Does the inclusion of canopy structure and elevation improve estimates of NEP and GEP compared with estimates obtained with meteorological variables only? Within a multiple linear regression, f_{cover} and elevation were combined with the meteorological driving variables RH, T_{soil}, and θ, and incoming PAR (the Landsberg approach) for each of the periods studied (Table 7). Canopy structure indicators and elevation covaried to some degree. Mean canopy height was strongly positively correlated with mean canopy depth (r = 0.94, p = 0.000) and f_{cover} (r = 0.64, p = 0.000),

Table 7. Multiple regression equations used to predict net ecosystem productivity (NEP) and gross ecosystem productivity (GEP) using meteorological variables, canopy fractional cover (f_{cover}), and elevation (Elev.), added to the results of the Landsberg equation (Table 6).

			p value of contribution				
	Period	Multiple regression equation	RH	T_{soil}	θ	f_{cover}	Elev.
NEP	P1	$NEP_r = 158 + 0.01RH - 1.54T_{soil} - 224\theta + 0.27Elev. + 9.95f_{cover}$	0.23	0.000	0.001	0.041	0.21
	P2	$NEP_r = -1.9 + 0.08RH - 1.44T_{soil} - 153\theta + 0.041Elev. + 8.36f_{cover}$	0.000	0.000	0.05	0.10	0.63
	P3	$NEP_r = 0.7 - 0.02RH - 1.60T_{soil} - 1091\theta + 0.17Elev. + 18.5f_{cover}$	0.25	0.004	0.36	0.020	0.32
GEP	P1	$GEP_r = 167 + 0.009RH - 0.84T_{soil} - 224\theta - 0.30Elev. + 10.45f_{cover}$	0.15	0.000	0.000	0.025	0.15
	P2	$GEP_r = -22.3 + 0.08RH - 0.88T_{soil} - 20.6\theta - 0.05Elev. + 8.88f_{cover}$	0.000	0.000	0.79	0.071	0.53
	P3	$GEP_r = 19.6 + 0.003RH - 0.84T_{soil} - 826\theta - 0.075Elev. + 16.4f_{cover}$	0.85	0.15	0.11	0.032	0.66

Note: RH, relative humidity; T_{soil}, soil temperature; θ, volumetric soil moisture. The relative importance of each contribution is indicated by the *p* value. Number of observations = 111 (P1), 166 (P2), and 126 (P3).

and canopy depth was correlated with f_{cover} ($r = 0.71$, $p = 0.000$). Canopy height was not significantly correlated with elevation ($r = 0.16$, $p = 0.07$), but f_{cover} tended to be negatively correlated with elevation ($r = -0.38$, $p = 0.000$). Of all the structural attributes, f_{cover} best described the variability in NEP and GEP. Modelled NEP and GEP, based on the multiple regression with the inclusion of meteorological variables, f_{cover}, and elevation, were compared with measured values in Fig. 8.

The inclusion of f_{cover} was sometimes a more important component of the flux than daily variability in θ (P3, and to a certain extent P2) and RH (P1 and P3) (Table 7). Elevation, however, was not an important part of the combined influence on fluxes, as demonstrated by the *p* values in Table 7. During most periods studied, f_{cover} improved predictions of NEP and GEP (when comparing r^2 and the root mean square error (RMSE) of Figs. 8 and 9). During P1, predictions of NEP and GEP were improved by 10% and 5%, respectively, when meteorological variables were included, and by an additional 15% and 4% when f_{cover} and elevation were included. Meteorological influences (apart from incoming PAR) were less important in P1 than in the other two periods. f_{cover} had a larger influence than meteorological driving variables on NEP (15% vs. 10%), but a slightly less important influence on GEP (4% vs. 5%). In P2, including additional parameters resulted in smaller improvements in the predictions, with the exception of the meteorological variables, which improved the Landsberg predicted NEP and GEP by 68% and 29% (NEP and GEP). Meteorological variables had a dominant influence on fluxes during P2, whereas f_{cover} and elevation had relatively minor influences, improving modelled NEP and GEP by an additional 3% and 11%, respectively. Much of the variability in fluxes during P2 remained unexplained, even after inclusion of meteorological variables and canopy structure and elevation. During P3, f_{cover} and elevation worsened the prediction of NEP by 16% compared with that modeled using meteorological driving variables alone (which improved NEP and GEP prediction by 28% and 4%), whereas GEP was only slightly improved by 4% when f_{cover} was included. Small improvements to modeled NEP and GEP from f_{cover} and elevation also resulted in lower RMSE.

On a daily basis rather than by study periods, canopy structure and elevation had varying correspondence with measured NEP and GEP (Fig. 9), perhaps because of sensitivity of fluxes to the vegetation characteristics of the maximum source area and available resources. We expect that areas with more biomass (e.g., foliage amounts) would be positively related to increased CO_2 uptake by vegetation because more leaves would be photosynthesizing. An assessment of light response curves during four days with similar meteorological conditions (7 and 8 July and 9 and 10 August), when fluxes came from opposite directions within the ecosystem, yields direct evidence of the influences of canopy structure and elevation on fluxes. On 7 July and 10 August, fluxes originated from the northwest part of the ecosystem: areas with relatively high leaf area, tall trees, and higher elevation. On 8 July and 9 August, fluxes originated from the east and southeast parts of the ecosystem: areas with relatively low leaf area, shorter trees, and low elevation. Light response curves for NEP and GEP on 7 July and 10 August (not shown) indicate that areas with more biomass, located at higher elevations, had greater ability to photosynthesize than areas with less biomass. A *t* test confirms that significant differences in light response curves exist between dates where fluxes originated from high biomass areas and dates where fluxes originated from low biomass areas ($p < 0.01$). Differences in Landsberg curve descriptors P_{max} and I_{comp} are demonstrated in Table 8 for specific dates.

Of the 22 days studied, 13 (59%) and 9 (41%) of the days showed significant ($p < 0.01$) positive relationships between increased biomass and increased NEP and GEP, respectively. Four and five additional days were also positively correlated with NEP and GEP, but did not have a significant influence. The opposite relationships were found on 5 and 8 days (NEP, GEP), where increased biomass was also related to increased atmospheric CO_2 concentrations, but only 2 and 3 days were significant ($p < 0.01$). The best correspondence between CO_2 uptake and increased biomass occurred during P1 and P3 when photosynthesis was not limited by θ, high mean T_{air}, and incoming PAR.

NEP and GEP were also significantly negatively affected by increased elevation (or vice versa) for 10 and 8 of 22 days, respectively (where $p < 0.01$) (Fig. 9). Negative relationships occurred mostly during P2 and P3, corresponding with high mean T_{air} and T_{soil}. For example, on 13 June 2002, GEP (and NEP) were negatively affected by fluxes originating from areas of higher elevation (Fig. 4). June 13 was also the warmest day of the week, with a mean T_{air} of 21.8 °C; mean T_{air} was 13.5 °C for the days prior to June 13 and 19.2 °C for the following days. Warmer days with increased T_{soil} typically resulted in a negative correspondence between elevation and CO_2 fluxes. In this case T_{soil} provides a gen-

Fig. 8. Relationships (adjusted r^2) between measured net ecosystem productivity (NEP) (*a*, *b*, and *c*) and gross ecosystem productivity (GEP) (*d*, *e*, and *f*), and modeled estimates of the NEP and GEP obtained with the Landsberg equation and multiple regression of the residuals presented in Table 6 (including f_{cover} and elevation) during three periods of study: 10–15 June 2002 (*a* and *d*), 5–13 July 2002 (*b* and *e*), and 7–13 August 2002 (*c* and *f*). Relationships are shown for periods between 0900 and 1700 hours local time.

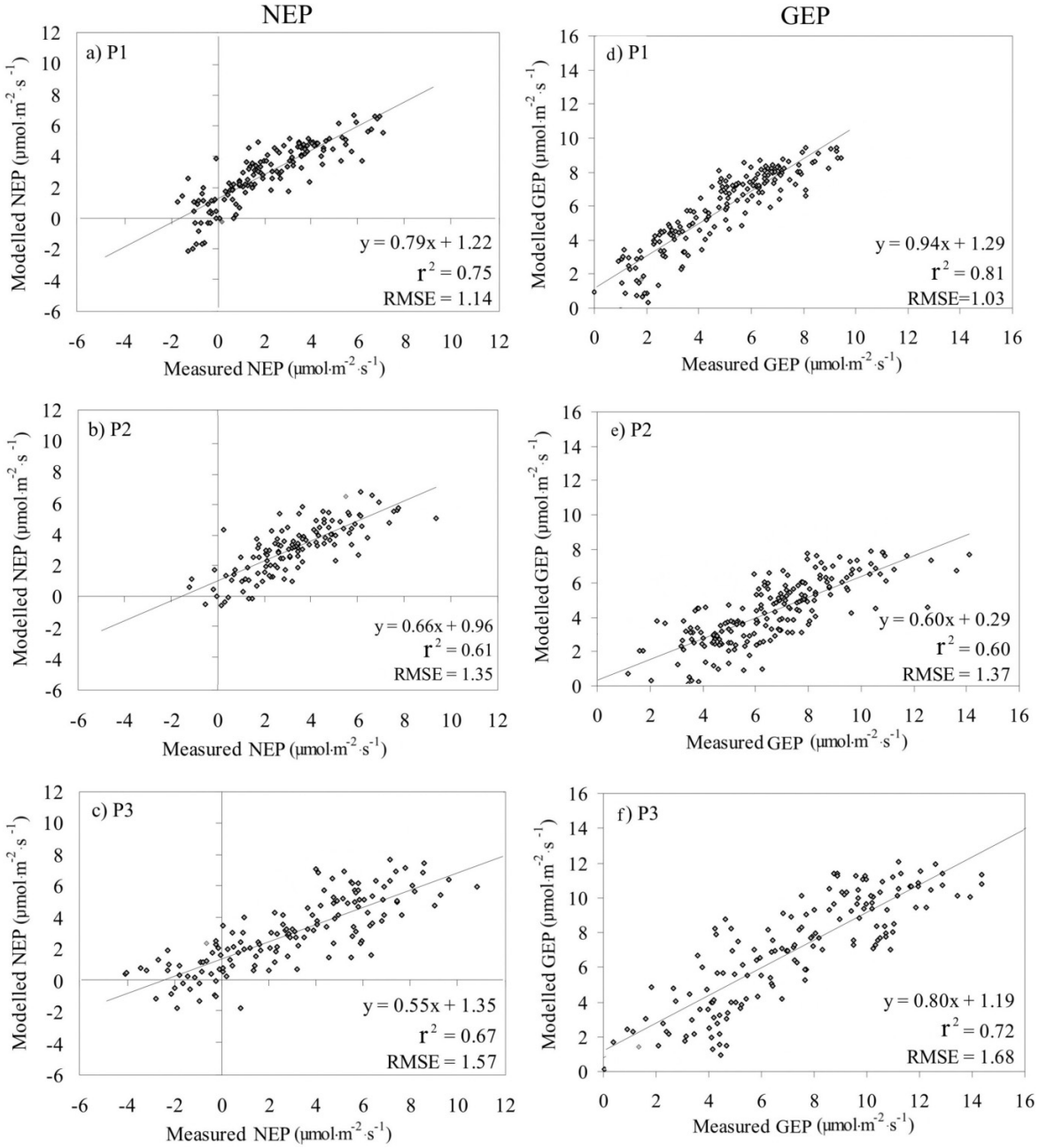

eral estimate of ecosystem T_{soil} variability over time because it is only measured in one location. Mean T_{air} and T_{soil} were greatest during P2 (T_{air} = 23.7 °C, T_{soil} = 14.4 °C) and P3 (T_{air} = 19.0 °C, T_{soil} = 14.3 °C) on days when elevation and NEP and GEP were significantly related. Cooler and wetter periods during P1 showed limited correspondence between CO_2 fluxes and elevation.

Discussion and conclusions

In this study, we found that CO_2 fluxes varied spatially and temporally as a result of variations in meteorological variables, canopy biomass, and elevation within a jack pine ecosystem. Why does the relative importance of interactions between CO_2 fluxes, and canopy structure and elevation vary on a daily basis and throughout each period? This may be due, in part, to sensitivity of fluxes to the characteristics of vegetation within the maximum source location of the fluxes and available resources. Footprint estimates indicate that the greatest contribution of measured fluxes typically originated from up to 150 to 300 m from the tower. Trees were typically shorter within 150 m east and southeast of the EC system (mean canopy height = 13.6 m), whereas trees were taller west and northwest of the tower (mean can-

Fig. 9. Bar graph of Pearson's *r* correlations between daily net ecosystem productivity (NEP) and gross ecosystem productivity (GEP), and (*a*) canopy fractional cover (f_{cover}) and (*b*) elevation ($n = \sim 17$ per day but may vary because of low surface friction velocity (u_*)). Orange and yellow bars represent p values <0.01. In Fig. 9*a*, 13 of 22 (NEP) and 9 of 22 (GEP) days are significantly correlated with areas of increased f_{cover}, whereas the opposite is found on 2 of 22 (NEP) and 3 of 22 (GEP) days. In Fig. 9*b*, 2 of 22 (NEP) and 3 of 22 (GEP) days are significantly correlated with areas of higher elevations, whereas 10 of 22 (NEP) and 8 of 22 (GEP) days are significantly correlated with areas of lower elevations. Increases in biomass (e.g., greater foliage) should be positively correlated with increased NEP and GEP.

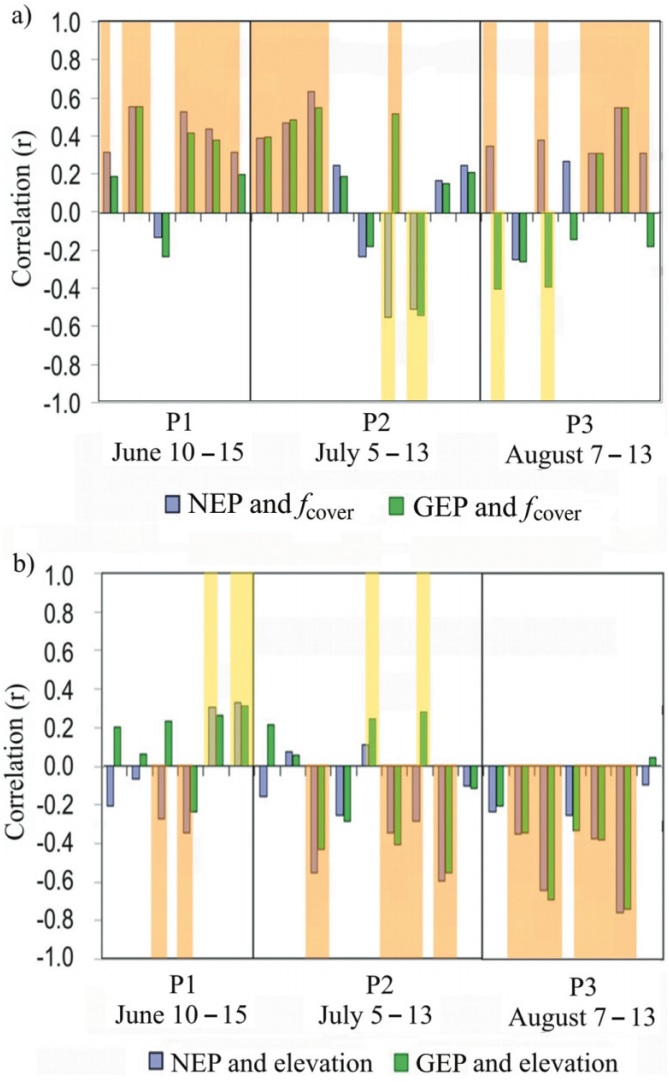

opy height = 15.2 m) (Fig. 1). Canopy f_{cover} was also low, ranging from 0.36 to 0.45 in all directions within 150 m of the EC.

At distances of 150 to 350 m of the EC, the ecosystem becomes more spatially variable. Mean tree heights ranged from 12.5 m (southeast of the EC) to 18.4 m (northwest of the EC), resulting in $\sim$32% difference in mean tree height within the two parts of the ecosystem from which CO_2 fluxes likely originated. f_{cover} also varied significantly, ranging between 0.36 and 0.81 at spatial resolutions of 1 m. The mean foliage fractional cover was higher to the northeast and northwest of the EC, and lower to the southeast and southwest of the site (Table 2). Even on a daily basis, the amount of biomass sampled by EC can vary greatly at OJP, depending on the source location of fluxes. Maximum source area locations can vary over space, as do vegetation and elevation characteristics. When vegetation and meteorological variables are combined, their effects on fluxes can also differ (Fig. 9). At OJP, Baldocchi et al. (2000) found that between 25% and 35% of incoming solar radiation reached the forest floor. Similarly, Griffis et al. (2003) suggested that approximately 70% of solar radiation was absorbed by the canopy at this site. In our study, spatial mapping of f_{cover} by airborne lidar at 1 m resolution showed that light penetration to the ground surface can be as little as 19% in areas of high f_{cover}, and as great as 64% in areas of low f_{cover}. These relatively large differences in the spatial variability of light absorption by canopies and penetration to the ground may explain the variable influences on CO_2 exchanges from different parts of the ecosystem. Future studies should examine the areal extent of classified f_{cover}, tree height, and elevation within footprints, not only footprint means, as examined in this study.

Over the course of several days, canopy structure and elevation exhibited strong influences on CO_2 fluxes during P1 and to a lesser extent during P3, but had relatively little influence during P2. This was perhaps because of limited availability of resources and saturation of photosynthesis by high amounts of mean incoming PAR. Canopy structural influences on CO_2 fluxes were typically less important than meteorological variables, but during many days, canopy structure, especially f_{cover}, explained a comparatively large proportion of the variance of NEP and GEP.

In this study, assessment of mean elevation within footprints was simplistic. For example, CO_2 fluxes may be affected by slope curvature, leading to either wetting or drying of soils, thereby affecting tree growth, photosynthesis, and R_e (e.g., Baldocchi et al. 1997; Baldocchi and Meyers 1998). Elevation is not necessarily indicative of microtopographic features affecting fluxes of CO_2 within the landscape because microtopography is also dependent on the spatial distribution of small hills and valleys, slope, and aspect. The effects of microtopographic features could be taken into account by incorporating local ground morphology, slope curvature (concave vs. convex), and aspect to properly classify upland and lowland areas and their attributes.

Based on this limited analysis and the variability in wind directions illustrated in Fig. 4 for the entire year of 2002, flux measurements at this site may not be equally measuring fluxes from all parts of the ecosystem surrounding the EC flux station. Winds typically originate from upland areas, which have slightly different canopy structural characteristics than low-lying areas. Differences in the variability in NEP could be influenced, to some degree, by differences in canopy and ground surface characteristics within the site. Rahman et al. (2001) found that EC underestimated gross CO_2 fluxes by 5% at OJP because biomass tended to be lower within the immediate vicinity of the EC than in the surrounding ecosystem (also found here). Fluxes at more heterogeneous sites may have an increased dependency on

Table 8. Net ecosystem productivity (NEP) and gross ecosystem productivity (GEP) light response curve characteristics for 4 days with similar meteorological conditions when footprints originated from opposite parts of the ecosystem (high biomass vs. low biomass (canopy fractional cover (f_{cover}), tree height), and higher elevation (upland) vs. lower elevation (lowland)).

	P_{max} ($\mu mol \cdot m^{-2} \cdot s^{-1}$)		I_{comp} ($\mu mol \cdot m^{-2} \cdot s^{-1}$)		Daily total flux ($\mu mol \cdot m^{-2} \cdot s^{-1}$)		
Date	NEP	GEP	NEP	GEP	NEP	GEP	Mean footprint characteristics
7 July 2002	3.1	7.5	450	273	44.9	166.8	High biomass, upland
8 July 2002	2.3	6.7	470	350	40.1	151.7	Low biomass, lowland
9 August 2002	5.8	9.7	390	125	87.3	194.4	Low biomass, lowland
10 August 2002	8.5	11.8	310	50	92.4	199.6	High biomass, upland

Note: P_{max}, maximum mean NEP (or GEP) at saturation; I_{comp}, light compensation point.

canopy structure and elevation. Along with meteorological variables, canopy structure and elevation may be a key factor in determining whether the annual carbon balance of a vegetated ecosystem is a net annual source or sink. Further research over extended (e.g., annual) periods is needed to determine if this is the case.

Acknowledgements

We would like to thank the Fluxnet-Canada Research Network and the Boreal Ecosystem Research and Monitoring Sites (BERMS) Project and all those individuals involved for collection and processing of flux data. We appreciate the efforts of the Applied Geomatics Research Group and C-CLEAR for collecting and processing at-cost lidar data and the National Water Research Institute (NWRI) for financially supporting part of the survey. Field data collection was performed with the aid of Bruce Davison, Chris Beasy, and Jordan Erker, and their efforts are appreciated. Jessika Töyra is acknowledged for her assistance with field validation and logistics. We appreciate the comments of two anonymous reviewers, Dr. P. Lafleur, Dr. P. Grogan, and Sonia Wharton for advice. Also, thank you to the late Werner Bauer (site manager) for his help and support. Funding for this project has been provided by CFCAS, NSERC, the BIOCAP Canada Foundation, and the Climate Research Division of Environment Canada. Laura Chasmer has been generously supported by graduate student scholarships from NSERC and OGSST.

References

Amiro, B.D. 1998. Footprint climatologies for evapotranspiration in a boreal catchment. Agric. For. Meteorol. **90**: 195–201. doi:10.1016/S0168-1923(97)00096-8.

Baldocchi, D.D., Vogel, C.A., and Hall, B. 1997. Seasonal variation of carbon dioxide exchange rates above and below a boreal jack pine forest. Agric. For. Meteorol. **83**: 147–170. doi:10.1016/S0168-1923(96)02335-0.

Baldocchi, D., and Meyers, T. 1998. On using eco-physiological, micrometeorological and biogeochemical theory to evaluate carbon dioxide, water vapor and trace gas fluxes over vegetation: a perspective. Agric. For. Meteorol. **90**: 1–25. doi:10.1016/S0168-1923(97)00072-5.

Baldocchi, D., Kelliher, F., Black, T.A., and Jarvis, P. 2000. Climate and vegetation controls on boreal zone energy exchange. Glob. Change Biol. **6**: 69–83. doi:10.1046/j.1365-2486.2000.06014.x.

Baldocchi, D. 2008. Turner Review No. 15: 'Breathing' of the terrestrial biosphere: lessons learned from a global network of carbon dioxide flux measurement systems. Aust. J. Bot. **56**: 1–26. doi:10.1071/BT07151.

Barr, A.G., Morgenstern, K., Black, T.A., McCaughey, J.H., and Nesic, Z. 2006. Surface energy balance closure by the eddy-covariance method above three boreal forest stands and implications for the measurement of the CO_2 flux. Agric. For. Meteorol. **140**: 322–337. doi:10.1016/j.agrformet.2006.08.007.

Chasmer, L., Hopkinson, C., Smith, B., and Treitz, P. 2006. Examining the influence of changing laser pulse repetition frequencies on conifer forest canopy returns. Photogramm. Eng. Remote Sensing, **72**: 1359–1367.

Chen, J., Falk, M., Euskirchen, E., Tha, K., Paw, U., Suchanek, T., Ustin, S., Bond, B., Brosofske, K., Phillips, N., and Bi, R. 2002. Biophysical controls of carbon flows in three successional Douglas-fir stands based on eddy-covariance measurements. Tree Physiol. **22**: 169–177. PMID:11830413.

Chen, J.M., Govind, A., Sonnentag, O., Zhang, Y., Barr, A., and Amiro, B. 2006. Leaf area index measurements at Fluxnet-Canada forest sites. Agric. For. Meteorol. **140**: 257–268. doi:10.1016/j.agrformet.2006.08.005.

Chen, B., Chen, J., Mo, G., Black, T.A., and Worthy, D.E. 2008. Comparison of regional carbon flux estimates from CO_2 concentration measurement and remote sensing based footprint integration. Global Biogeochem. Cycles, **22**(GB2012). doi:10.1029/2007GB003024.

Choudhury, B., and Monteith, J. 1988. A four-layer model for the heat budget of homogeneous land surfaces. Q.J.R. Meteorol. Soc. **114**: 373–398. doi:10.1002/qj.49711448006.

Fluxnet-Canada. 2003. Fluxnet-Canada measurement protocols. Working draft version 1.3. Fluxnet-Canada Network Management Office, Laval, Que. Available from http://www.fluxnet-canada.ca [accessed xxxxx]..

Foken, T., and Leclerc, M.Y. 2004. Methods and limitations in validation of footprint models. Agric. For. Meteorol. **127**: 223–234. doi:10.1016/j.agrformet.2004.07.015.

Goetz, S., Prince, S., Goward, S., Thawley, M., Small, J., and Johnston, A. 1999. Mapping net primary production and related biophysical variables with remote sensing: Application to the BOREAS region. J. Geophys. Res. **104**(D22): 27 719 – 27 734. doi:10.1029/1999JD900269.

Gower, S., Vogel, V., Norman, J., Kucharik, C., Steele, S., and Stow, T. 1997. Carbon distribution and aboveground net primary production of aspen, jack pine, and black spruce stands in Saskatchewan and Manitoba, Canada. J. Geophys. Res. **102**: 29 029 – 29 041. doi:10.1029/97JD02317.

Griffis, T.J., Black, T.A., Morgenstern, K., Barr, A.G., Nesic, Z., Drewitt, G.B., Gaumont-Guay, D., and McCaughey, J.H. 2003. Ecophysiological controls on the carbon balances of three south-

ern boreal forests. Agric. For. Meteorol. **117**: 53–71. doi:10.1016/S0168-1923(03)00023-6.

Gryning, S.E., Holtslag, A., Irwin, J.S., and Silvertsen, B. 1987. Applied dispersion modeling based on meteorological scaling parameters. Atmos. Environ. **21**: 79–89. doi:10.1016/0004-6981(87)90273-3.

Heinsch, F.A., Zhao, M., Running, S., Kimball, J., Nemani, R., Davis, K., Bolstad, P., Cook, B., Desai, A., Ricciuto, D., Law, B., Oechel, W., Kwon, H., Luo, H., Wofsy, S., Dunn, A., Munger, J.W., Baldocchi, D., Xu, L., Hollinger, D., Richardson, A., Stoy, P., Siqueira, M., Monson, R., Burns, S., and Flanagan, L. 2006. Evaluation of remote sensing based terrestrial productivity from MODIS using regional tower eddy flux network observations. IEEE Trans. Geosci. Rem. Sens. **44**: 1908–1925. doi:10.1109/TGRS.2005.853936.

Hollinger, D.Y., Goltz, S.M., Davidson, E.A., Lee, J.T., Tu, K., and Valentine, H.T. 1999. Seasonal patterns and environmental control of carbon dioxide and water vapour exchange in an ecotonal boreal forest. Glob. Change Biol. **5**: 891–902. doi:10.1046/j.1365-2486.1999.00281.x.

Kim, J., Guo, Q., Baldocchi, D., Leclerc, M., Xu, L., and Schmid, H. 2006. Upscaling fluxes from tower to landscape: Overlaying flux footprints on high-resolution (IKONOS) images of vegetation cover. Agric. For. Meteorol. **136**: 132–146. doi:10.1016/j.agrformet.2004.11.015.

Kljun, N., Calanca, P., Rotach, M., and Schmid, H. 2004. A simple parameterisation for flux footprint predictions. Boundary-Layer Meteorol. **112**: 503–523. doi:10.1023/B:BOUN.0000030653.71031.96.

Kljun, N., Black, T.A., Griffis, T.J., Barr, A.G., Gaumont-Guay, D., Morgenstern, K., McCaughey, J.H., and Nesic, Z. 2006. Response of net ecosystem productivity of three boreal forest stands to drought. Ecosystems (N. Y., Print), **9**: 1128–1144. doi:10.1007/s10021-005-0082-x.

Landsberg, J.J., and Waring, R.H. 1997. A generalized model of forest productivity using simplified concepts of radiation-use efficiency, carbon balance and partitioning. For. Ecol. Manage. **95**: 209–228. doi:10.1016/S0378-1127(97)00026-1.

Leblanc, S., Chen, J., Fernandes, R., Deering, D., and Conley, A. 2005. Methodology comparison for canopy structure parameters extraction from digital hemispherical photography in boreal forests. Agric. For. Meteorol. **129**: 187–207. doi:10.1016/j.agrformet.2004.09.006.

Lim, K., and Treitz, P. 2004. Estimation of aboveground forest biomass from airborne discrete return laser scanner data using canopy-based quantile estimators. Scand. J. For. Res. **19**: 558–570. doi:10.1080/02827580410019490.

Massman, W.J., and Lee, X. 2002. Eddy covariance flux corrections and uncertainties in long term studies of carbon and energy exchange. Agric. For. Meteorol. **113**: 121–144. doi:10.1016/S0168-1923(02)00105-3.

Middleton, E.M., Sullivan, J., Bovard, B., Deluca, A., Chan, S., and Cannon, T. 1997. Seasonal variability in foliar characteristics and physiology for boreal forest species at five Saskatchewan tower sites during the 1994 Boreal Ecosystem–Atmosphere Study. J. Geophys. Res. **102**(D24): 28831–28844. doi:10.1029/97JD02560.

Monteith, J., and Unsworth, M. 1990. Principles of Environmental Physics. 2nd ed. Edward Arnold, New York.

Morsdorf, F., Kötz, B., Meier, E., Itten, K., and Allgöwer, B. 2006. Estimation of LAI and fractional cover from small footprint airborne laser scanning data based on gap fraction. Sens. Environ. **104**: 50–61. doi:10.1016/j.rse.2006.04.019.

Rahman, A., Gamon, J., Fuentes, D., Roberts, D., and Prentiss, D. 2001. Modeling spatially distributed ecosystem flux of boreal forest using hyperspectral indices from AVIRIS imagery. J. Geophys. Res. **106**(D24): 33 579 – 33 591. doi:10.1029/2001JD900157.

Shuttleworth, W., and Wallace, J. 1985. Evaporation from sparse crops — an energy combination theory. Q. J. R. Meteorol. Soc. **111**: 839–855. doi:10.1256/smsqj.46909.

Turner, D.P., Urbanski, S., Bremer, D., Wofsy, S., Meyers, T., Gower, S., and Gregory, M. 2003. A cross-biome comparison of daily light use efficiency for gross primary production. Glob. Change Biol. **9**: 383–395. doi:10.1046/j.1365-2486.2003.00573.x.

Vesala, T., Kljun, N., Rannik, U., Rinne, J., Sogachev, A., Markkanen, T., Sabelfeld, K., Foken, Th., and Leclerc, M.Y. 2008. Flux and concentration footprint modelling: State of the art. Environ. Pollut. **152**: 666. doi:10.1016/j.envpol.2007.06.070.

Wilson, K.B., Goldstein, A., Falge, E., Aubinet, M., Baldocchi, D., Berbigier, P., Bernhofer, C., Ceulemans, R., Dolman, H., Field, C., Grelle, A., Ibrom, A., Law, B.E., Kowalski, A., Meyers, T., Moncrieff, J., Monson, R., Oechel, W., Tenhunen, J., Valentini, R., and Verma, S. 2002. Energy balance closure at FLUXNET sites. Agric. For. Meteorol. **113**: 223–243. doi:10.1016/S0168-1923(02)00109-0.

Yang, P.C., Black, T.A., Neumann, H.H., Novak, M.D., and Blanken, P.D. 1999. Spatial and temporal variability of CO_2 concentration and flux in a boreal aspen forest. J. Geophys. Res. **104**: 27 653 – 27 661. doi:10.1029/1999JD900295.

Zhang, Y., Chen, J., and Miller, J. 2005. Determining digital hemispherical photograph exposure for leaf area index estimation. Agric. For. Meteorol. **133**: 166–181. doi:10.1016/j.agrformet.2005.09.009.